Proton motion inside $[(DMF)_2H]_2[W_6Cl_{14}]$: structural, Raman and luminescence studies

Boris A. Kolesov†, Anastasia V. Chupina†,‡, Aleksey S. Berezin†, Nikolay B. Kompankov†, Pavel A. Abramov†,‖, Maxim N. Sokolov†*

Supporting Information

Table of Contents

Part A. Synthesis and characterization

General information

$(H_7O_3)_2[W_6Cl_{14}]\cdot 3H_2O$ was synthesized according to the literature.[1,2] IR spectrum was recorded on a Bruker Scimitar spectrometer. Solid state NMR experiments were run on a Bruker Avance III 500 spectrometer at 5 – 12 KHz.

Raman spectroscopy

The Raman spectra were collected on a LabRAM Horiba single stage spectrometer with a CCD Symphony (Jobin Yvon) detector with 2048 horizontal pixels. The laser power (633 nm line of He-Ne laser) at the sample was typically less than 0.1 mW. The spectra at all temperatures were measured in backscattering collection geometry with a Raman microscope. The powder was fixed on the cold finger of the cryostat. The spectral resolution was 0.7 cm^{-1}. The laser emission line at 6.83 cm^{-1} was used to correct low-wavenumber spectra (< 300 cm^{-1}).

Luminescence

Corrected luminescence spectra were recorded on a Fluorolog 3 spectrometers (Horiba Jobin Yvon) with a R928 (FL-1073) photomultiplier and two Czerny–Turner double monochromators. Temperature dependences of luminescence were studied out using Optistat DN optical cryostat (Oxford Instruments).

DFT calculations

The geometry optimizations followed by frequency calculations were made for the two $[(DMF)_2H]^+$ dimeric isomers with intermolecular O···H–O bonds using the Amsterdam density functional (ADF2017, SCM, Theoretical Chemistry, Vrije Universiteit, Amsterdam, The Netherlands, http://www.scm.com)[3,4] program with a gradient exchange functional GGA (BP86 – Becke[5] and Perdew[6]). Triple zeta basis sets and the no frozen core approximation are used in all the calculations.

References:

(1) Fedin, V. P.; Gerasko, O. A.; Fedorov, V. E.; Slovokhotov, Y.L. Struchkov, Y. T. Syntheses and Structure of Chloride Clusters of Molybdenum. *Izv. Sib. Otd. Akad. Nauk SSSR SERIYA KHIMICHESKIKH Nauk* **1988**, No. 6, 64–70.

(2) Abramov, P. A.; Rogachev, A. V.; Mikhailov, M. A.; Virovets, A. V.; Peresypkina, E. V.; Sokolov, M. N.; Fedin, V. P. Hexanuclear Chloride and Brimode Tungsten Clusters and Their Derivatives. *Russ. J. Coord. Chem.* **2014**, *40* (5), 259–267.

(3) te Velde, G.; Bickelhaupt, F. M.; Baerends, E. J.; Fonseca Guerra, C.; van Gisbergen, S. J. A.; Snijders, J. G.; Ziegler, T. Chemistry with ADF. *J. Comput. Chem.* **2001**, *22* (9), 931–967.

(4) Fonseca Guerra, C.; Snijders, J. G.; te Velde, G.; Baerends, E. J. Towards an Order- N DFT Method. *Theor. Chem. Accounts Theory, Comput. Model. (Theoretica Chim. Acta)* **1998**, *99* (6), 391–403.

(5) Becke, A. D. Density-Functional Exchange-Energy Approximation with Correct Asymptotic Behavior. *Phys. Rev. A* **1988**, *38* (6), 3098–3100.

(6) Perdew, J. P. Density-Functional Approximation for the Correlation Energy of the Inhomogeneous Electron Gas. *Phys. Rev. B* **1986**, *33* (12), 8822–8824.

Synthesis of $[(DMF)_2H]_2[W_6Cl_{14}]$ (1):

0.200 g (0.122 mmol) $(H_7O)_3[W_6Cl_{14}]\cdot 3H_2O$ was dissolved with stirring in 5 mL of DMF for 10 minutes. When 50 mL of diethyl ether was added to the resulting solution, a precipitate formed. The resulting mixture was centrifuged, the solution was decanted, the residue was dried in air. The resulting bright yellow substance was dissolved in 1 mL of CH_2Cl_2 and left to evaporate in air for several hours. Yield: 0.144 g (72%). Analysis found C, H, N (%): 7.5, 1.7, 2.9; calcd. for $C_{12}H_{30}Cl_{14}N_4O_4W_6$ C, H, N (%): 7.6, 1.6, 3.0.

IR (oil, cm^{-1}): 2922(w), 2845(w), 1306(s, sh), 1228(vs), 1154(s), 1059(m), 1022(m), 976(m), 927(m), 727(m), 692(m), 652(m), 620(m), 593(m), 522(m).

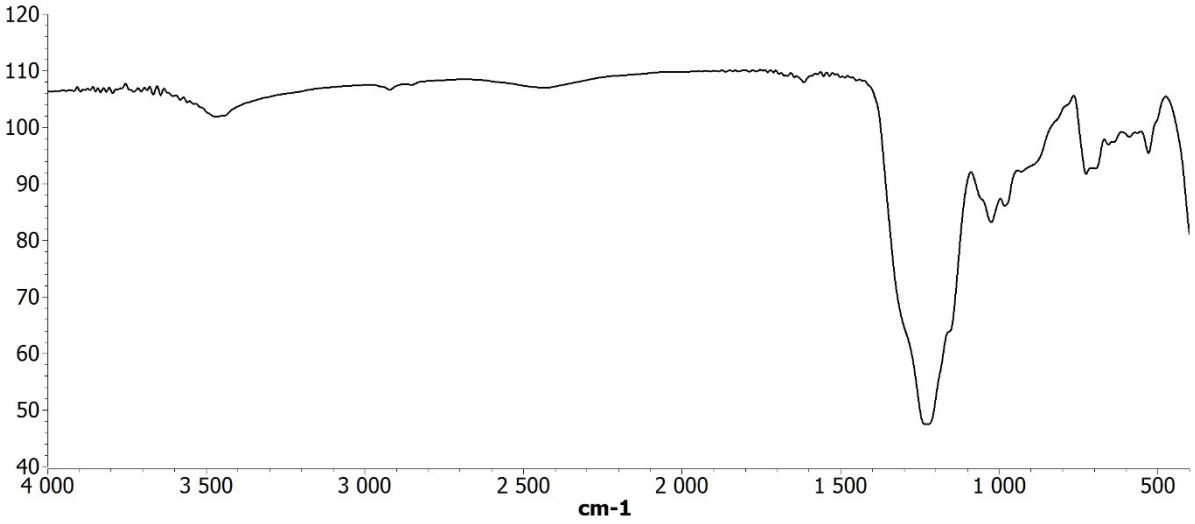

Fig. S1. IR spectrum of 1 in oil.

Part B. Structural data

X-ray crystallography.

Crystallographic data and refinement details for **1** are given in Table S1. For all structures: $C_{12}H_{30}Cl_{14}N_4O_4W_6$, M_r = 1893.80, monoclinic, $P2_1/n$, Z = 2.

The diffraction data were collected on a Bruker D8 Venture diffractometer with a CMOS PHOTON III detector and IμS 3.0 source (Mo Kα radiation, λ = 0.71073 Å) at 85 K and 298 K. The ϕ- and ω-scan techniques were employed. Absorption correction was applied by SADABS (Bruker Apex3 software suite: Apex3, SADABS-2016/2 and SAINT, version 2018.7-2; Bruker AXS Inc.: Madison, WI, 2017.).

The diffraction data were collected on a New Xcalibur (Agilent Technologies) diffractometer with MoK_α radiation (λ = 0.71073) by doing ϕ scans of narrow (0.5°) frames at 140 K. Absorption correction was done empirically using SCALE3 ABSPACK (CrysAlisPro, Agilent Technologies, Version 1.171.37.35 (release 13-08-2014 CrysAlis171 .NET)).

Structures were solved by SHELXT[7] and refined by full-matrix least-squares treatment against $|F|^2$ in anisotropic approximation with SHELX 2014/7[8] in ShelXle program.[9] H-atoms were refined in the geometrically calculated positions. The proton between DMF molecules was not directly localized and added to the complex composition.

The crystallographic data have been deposed in the Cambridge Crystallographic Data Centre under the deposition codes CCDC 2020091 (85 K), 2020092 (140 K), 2020093 (298 K).

XRPD

XRD analysis of polycrystals was performed on Shimadzu XRD-7000 diffractometer (CuK-alpha radiation, Ni – filter, linear One Sight detector, 5 – 70° 2θ range, 0.0143° 2θ step, 2s per step).

References:

(7) Sheldrick, G. M. SHELXT – Integrated Space-Group and Crystal-Structure Determination. *Acta Crystallogr. Sect. A Found. Adv.* **2015**, *71* (1), 3–8.

(8) Sheldrick, G. M. Crystal Structure Refinement with SHELXL. *Acta Crystallogr. Sect. C Struct. Chem.* **2015**, *71* (1), 3–8.

(9) Hübschle, C. B.; Sheldrick, G. M.; Dittrich, B. ShelXle : A Qt Graphical User Interface for SHELXL. *J. Appl. Crystallogr.* **2011**, *44* (6), 1281–1284.

Table S1. XRD Experimental details for 1.

Temperature (K)	85	140	298
a, *b*, *c* (Å)	10.6059 (3), 10.3846 (3), 17.1139 (5)	10.6198 (8), 10.3883 (8), 17.0912 (10)	10.892 (4), 10.536 (3), 17.354 (6)
b (°)	96.948 (1)	97.256 (7)	98.397 (12)
V (Å^3)	1871.05 (9)	1870.4 (2)	1970.3 (11)
μ (mm^{-1})	19.40	19.40	18.42
Crystal size (mm)	0.12 × 0.08 × 0.05	0.12 × 0.10 × 0.10	0.11 × 0.10 × 0.10
Diffractometer	Bruker D8 Venture	New Xcalibur, AtlasS2	Bruker D8 Venture
Absorption correction	Multi-scan *SADABS* (Bruker-AXS, 2004)	Multi-scan *CrysAlis PRO* 1.171.38.41 (Rigaku Oxford Diffraction, 2015) Empirical absorption correction using spherical harmonics, implemented in SCALE3 ABSPACK scaling algorithm.	Multi-scan *SADABS* (Bruker-AXS, 2004)
T_{min}, T_{max}	0.510, 0.746	0.537, 1.000	0.294, 0.491
No. of measured, independent and observed [$I > 2\sigma(I)$] reflections	49924, 5693, 5204	9601, 4466, 3579	19649, 4274, 3358
R_{int}	0.041	0.026	0.045
θ values (°)	θ_{max} = 30.5, θ_{min} = 2.8	θ_{max} = 29.5, θ_{min} = 3.5	θ_{max} = 27.0, θ_{min} = 2.8
$(\sin\theta/\lambda)_{max}$ (Å^{-1})	0.714	0.693	0.640
Range of *h*, *k*, *l*	-15 ≤ *h* ≤ 15, -14 ≤ *k* ≤ 14, -24 ≤ *l* ≤ 23	-13 ≤ *h* ≤ 14, -12 ≤ *k* ≤ 13, -16 ≤ *l* ≤ 23	-13 ≤ *h* ≤ 13, -13 ≤ *k* ≤ 13, -22 ≤ *l* ≤ 22
$R[F^2 > 2\sigma(F^2)]$, $wR(F^2)$, *S*	0.021, 0.045, 1.09	0.031, 0.063, 1.01	0.030, 0.062, 1.02
No. of reflections, parameters, restraints	5693, 179, 0	4466, 179, 0	4274, 179, 0
Weighting scheme	$w = 1/[\sigma^2(F_o^2) + (0.0075P)^2 + 7.6064P]$ where $P = (F_o^2 + 2F_c^2)/3$	$w = 1/[\sigma^2(F_o^2) + (0.0233P)^2]$ where $P = (F_o^2 + 2F_c^2)/3$	$w = 1/[\sigma^2(F_o^2) + (0.0188P)^2 + 1.3999P]$ where $P = (F_o^2 + 2F_c^2)/3$
$\Delta\rho_{max}$, $\Delta\rho_{min}$ (e Å^{-3})	1.55, -1.64	1.61, -1.89	0.80, -0.90

Computer programs: *APEX2* (Bruker-AXS, 2004), *CrysAlis PRO* 1.171.38.41 (Rigaku OD, 2015), *SAINT* (Bruker-AXS, 2004), *SHELXS2014* (Sheldrick, 2014), *SHELXL2014* (Sheldrick, 2014), ShelXle (Hübschle, 2011), CIFTAB-2014 (Sheldrick, 2014).

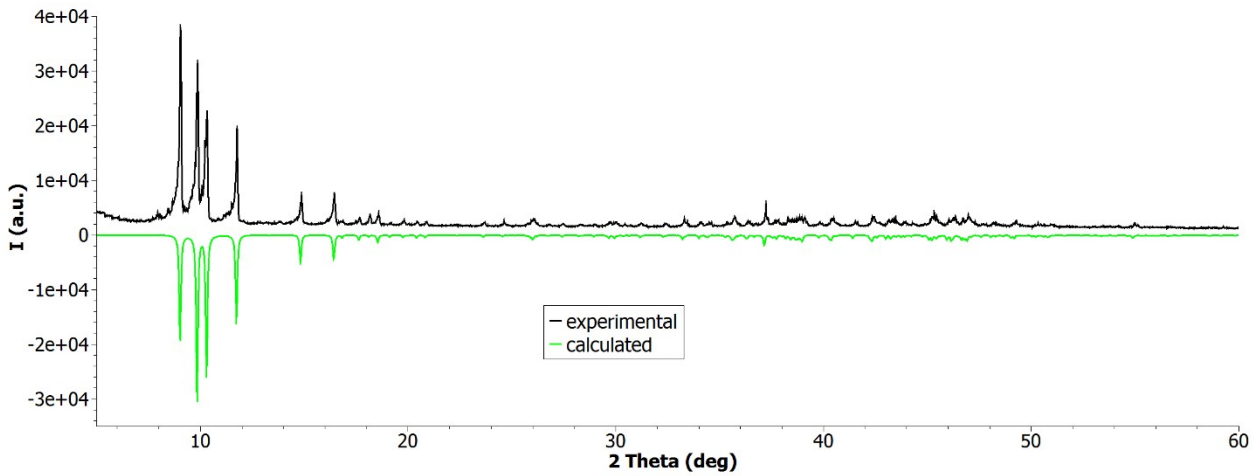

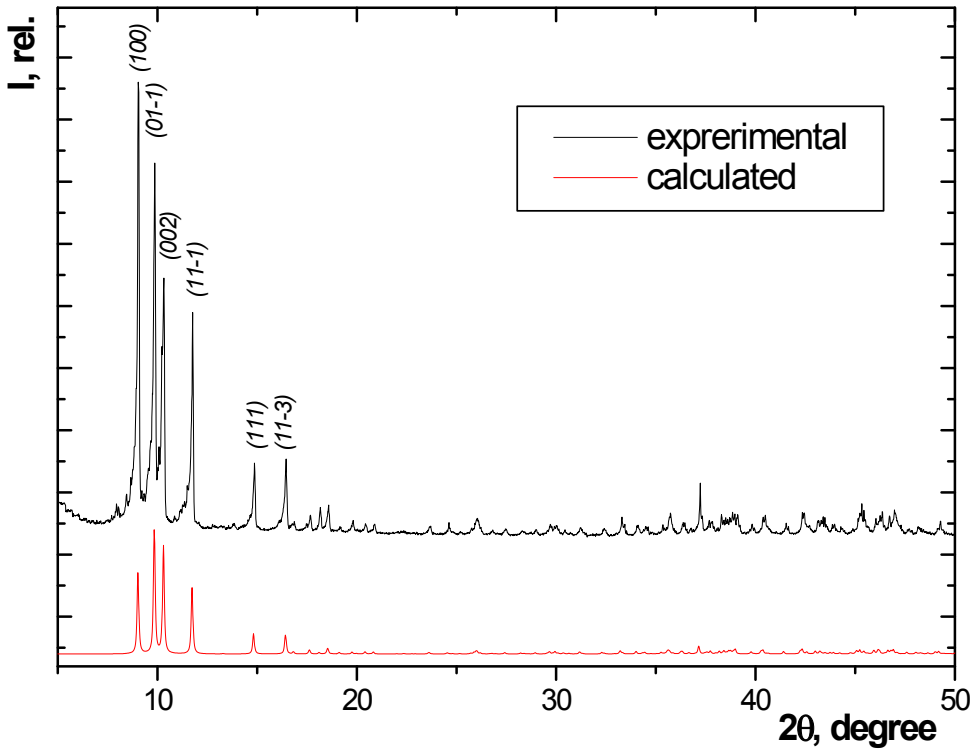

Fig. S2. Powder X-ray diffraction pattern comparison for **1** (top) and Miller indices for XRPD data (bottom).

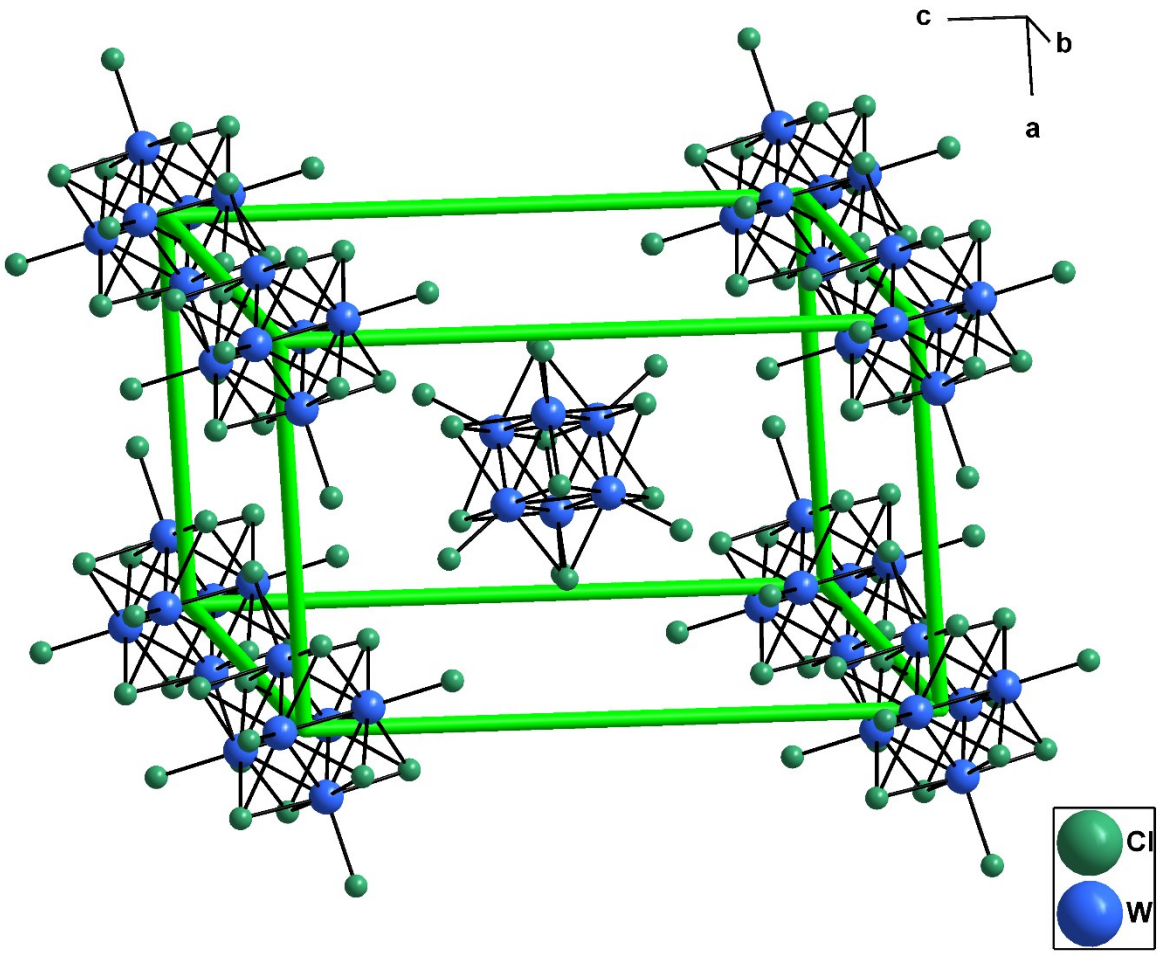

Fig. S3. Bcc-type of $[W_6Cl_{14}]^{2-}$ sublattice.

Part C. Bond distances analysis

Statistical analysis:

Min 2.104

Max 2.887

Mean 2.575

Std Dev. 0.216

Min Dev 0.189

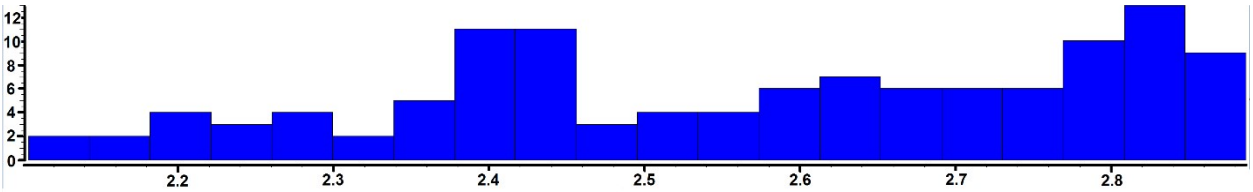

Fig. S4. Histogram of O…O distances between two DMF molecules from CCDC.

Table S2. List of the search results

Identifier	NAME	DIST3
search3|BOXPOW|0	BOXPOW	2.597
search3|BOXQAJ|1	BOXQAJ	2.374
search3|BOXQIR|2	BOXQIR	2.719
search3|COXXAR|3	COXXAR	2.882
search3|GOZJIR|4	GOZJIR	2.754
search3|KUHKOQ|5	KUHKOQ	2.441
search3|QOXSEE|6	QOXSEE	2.833
search3|QOXVEH|7	QOXVEH	2.758
search3|AXODOI|8	AXODOI	2.789
search3|BEPREV|9	BEPREV	2.65
search3|BEPREV02|10	BEPREV02	2.611
search3|BOQKEA|11	BOQKEA	2.402
search3|BOWZOD|12	BOWZOD	2.555
search3|CANXEW|13	CANXEW	2.386
search3|CEGQUB|14	CEGQUB	2.817
search3|CISXEJ|15	CISXEJ	2.769
search3|CIXRIK|16	CIXRIK	2.442
search3|COBPOB|17	COBPOB	2.585
search3|COQGAS|18	COQGAS	2.5
search3|DADZOA|19	DADZOA	2.226
search3|DAPPIV|20	DAPPIV	2.654
search3|DIKFAF|21	DIKFAF	2.374

search3|DUVNIS01|22	DUVNIS01	2.828
search3|EHEHOP|23	EHEHOP	2.283
search3|ESUVAR01|24	ESUVAR01	2.885
search3|ESUVAR02|25	ESUVAR02	2.45
search3|ETIXAI|26	ETIXAI	2.652
search3|FERCIR|27	FERCIR	2.818
search3|FIDQOZ|28	FIDQOZ	2.696
search3|FUNREM|29	FUNREM	2.438
search3|FUZXEF|30	FUZXEF	2.39
search3|GASMUL|31	GASMUL	2.176
search3|GIMTIH|32	GIMTIH	2.262
search3|GOJQIG|33	GOJQIG	2.839
search3|GOQCOG|34	GOQCOG	2.77
search3|HOFQIE|35	HOFQIE	2.797
search3|HUCGAO|36	HUCGAO	2.67
search3|IGINIX|37	IGINIX	2.457
search3|ILIVIJ|38	ILIVIJ	2.887
search3|IWAJIA|39	IWAJIA	2.642
search3|IWESOT|40	IWESOT	2.806
search3|JAPSOI|41	JAPSOI	2.104
search3|JINNEZ|42	JINNEZ	2.414
search3|KAVNIH|43	KAVNIH	2.816
search3|KENWUV|44	KENWUV	2.431
search3|KENXAC|45	KENXAC	2.389
search3|KENXEG|46	KENXEG	2.364
search3|KENXIK|47	KENXIK	2.423
search3|KENXUW|48	KENXUW	2.353
search3|KENYAD|49	KENYAD	2.425
search3|KOXGOV|50	KOXGOV	2.865
search3|KUTCUZ|51	KUTCUZ	2.581
search3|LAXZUF|52	LAXZUF	2.676
search3|LAZKUU|53	LAZKUU	2.804
search3|LELROL|54	LELROL	2.756
search3|LIWHUW|55	LIWHUW	2.138
search3|LIXJEJ|56	LIXJEJ	2.467
search3|LIXWIB|57	LIXWIB	2.637
search3|LUNTAQ|58	LUNTAQ	2.796
search3|LUYCAK|59	LUYCAK	2.385
search3|MIJMEY|60	MIJMEY	2.575
search3|MIPHAW|61	MIPHAW	2.423
search3|MOMJED|62	MOMJED	2.221
search3|MONBEX|63	MONBEX	2.667
search3|NABLEK|64	NABLEK	2.655
search3|NAKGOW|65	NAKGOW	2.23

search3|NAZPIP|66	NAZPIP	2.779
search3|NUYNEC|67	NUYNEC	2.472
search3|OCEVEX|68	OCEVEX	2.56
search3|OCEVEX01|69	OCEVEX01	2.541
search3|OMEYEL|70	OMEYEL	2.698
search3|OSOFOS|71	OSOFOS	2.764
search3|PAKXIK|72	PAKXIK	2.312
search3|PEVGEF|73	PEVGEF	2.627
search3|PIVBUT|74	PIVBUT	2.699
search3|POHCOG|75	POHCOG	2.164
search3|POWRAU|76	POWRAU	2.207
search3|PUVHIZ|77	PUVHIZ	2.819
search3|QAYHED|78	QAYHED	2.738
search3|QOCXIS|79	QOCXIS	2.376
search3|QOPZIF|80	QOPZIF	2.203
search3|QUMFUB|81	QUMFUB	2.73
search3|RAKGES|82	RAKGES	2.497
search3|RAZQAL|83	RAZQAL	2.595
search3|REBPEW|84	REBPEW	2.851
search3|RECFAM|85	RECFAM	2.387
search3|REPDUN|86	REPDUN	2.81
search3|RIFREF|87	RIFREF	2.778
search3|RIHGUL|88	RIHGUL	2.68
search3|RIJHAW|89	RIJHAW	2.527
search3|ROYSIJ|90	ROYSIJ	2.877
search3|ROYSOP|91	ROYSOP	2.847
search3|ROYSUV|92	ROYSUV	2.847
search3|ROYTAC|93	ROYTAC	2.859
search3|SIQFEE|94	SIQFEE	2.832
search3|SIQFEE01|95	SIQFEE01	2.805
search3|SOWVEH|96	SOWVEH	2.562
search3|TAZGEI|97	TAZGEI	2.331
search3|TIZPOI02|98	TIZPOI02	2.208
search3|TUCREQ|99	TUCREQ	2.256
search3|UGOHUT|100	UGOHUT	2.379
search3|UKUQAT|101	UKUQAT	2.437
search3|USOXEH|102	USOXEH	2.262
search3|WAPSOY|103	WAPSOY	2.412
search3|WAPSOY|104	WAPSOY	2.428
search3|WAPSOY|105	WAPSOY	2.431
search3|WAPSOY|106	WAPSOY	2.411
search3|WAPSOY|107	WAPSOY	2.413
search3|WAQGOM|108	WAQGOM	2.852
search3|WAYKAK|109	WAYKAK	2.625

search3|WEXYOP|110	WEXYOP	2.516
search3|WIRMOB|111	WIRMOB	2.802
search3|XODDAY|112	XODDAY	2.825
search3|XUCRUK|113	XUCRUK	2.281
search3|XUPCES|114	XUPCES	2.649
search3|YUDFIO|115	YUDFIO	2.826
search3|YUDFOU|116	YUDFOU	2.875
search3|YUSGEY|117	YUSGEY	2.728

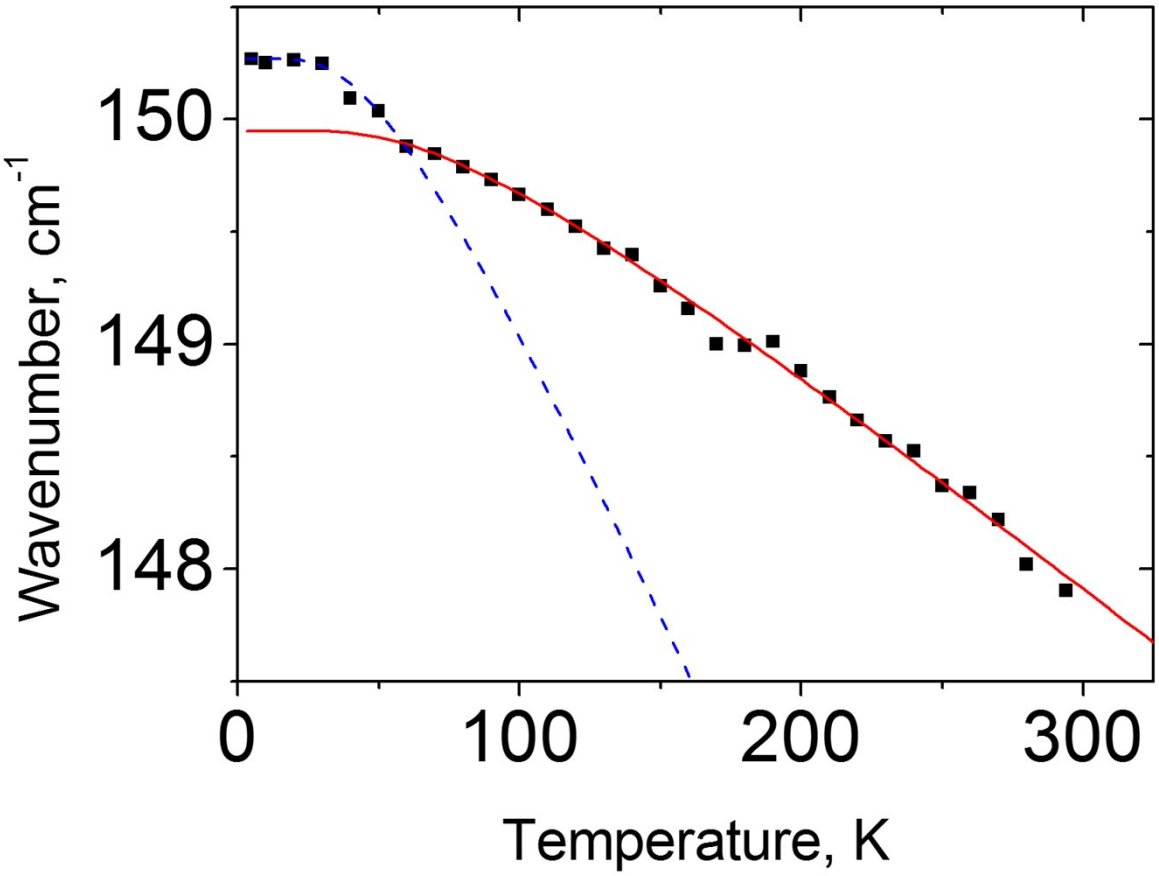

Fig. S5. Temperature dependence of the position of the maximum of the 150 cm^{-1} mode, presumably related to the molecule-to-molecule translational vibrations of a long hydrogen bond. The low-temperature fitting dashed curve is described by the excitation of the ~100 cm^{-1} mode of lattice vibrations, and the high-temperature solid curve is described by the excitation of the 150 cm^{-1} phonon itself.

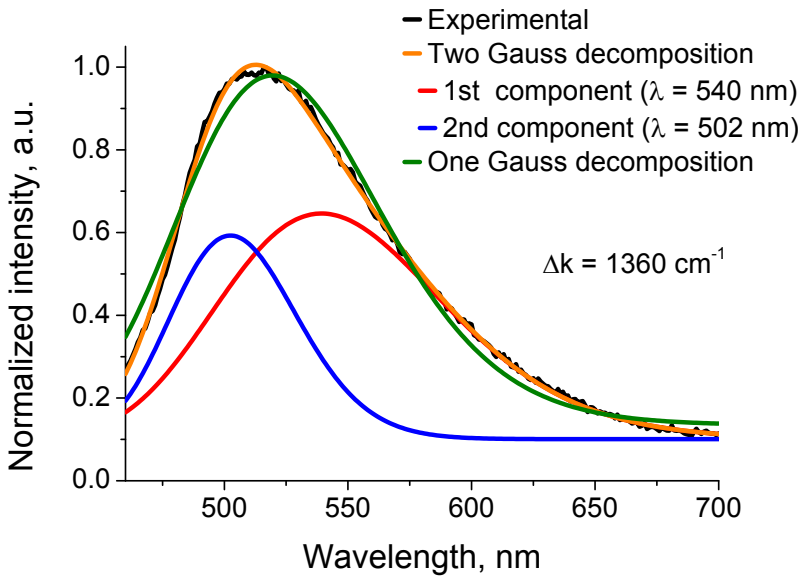

Fig. S6. The comparison of the experimental PL (λ_{Em} = 450 nm) spectra of **1** at 77 K and the decomposition of the spectrum in the direct energy scale using one and two Gauss functions.

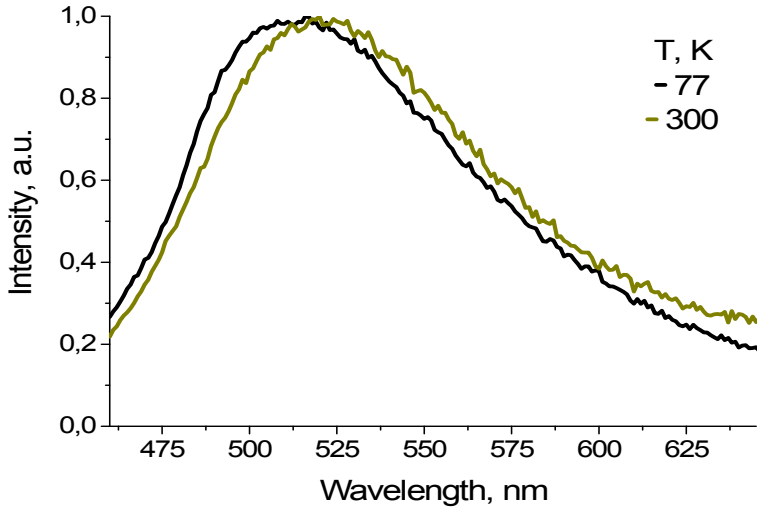

Fig. S7. Normalized PL (λ_{Em} = 450 nm) spectra of **1** at 77 K and 300 K.